Coupling Between Transmission Line Antennas: Analytic Solution, FDTD, and Measurements

Stavros V. Georgakopoulos, *Student Member, IEEE*, Constantine A. Balanis, *Fellow, IEEE*, and Craig R. Birtcher

***Abstract*—Transmission line antennas are widely used elements. Analytical formulations for the coupling between transmission line antennas, e.g., loops and inverted-L's, are developed. Furthermore, corrected current distributions that exhibit nonzero input current at the antiresonances of such elements are derived. The analytical results are compared with finite-difference time-domain (FDTD) calculations and measurements. Also, the physics of coupling is discussed. Finally, an FDTD technique that efficiently computes the two-port network parameters of a system of two antennas is developed based on a source with an internal resistance.**

***Index Terms*—FDTD methods, mutual coupling, transmission line antennas.**

I. Introduction

TRANSMISSION line antennas are widely used wire antennas. Due to their low profile they find a variety of applications in different areas of communications such as missile telemetry, mobile telephony, aeronautical mobile communications, and airborne platforms (such as helicopters, airplanes, missiles, etc.). Different shapes and configurations such as inverted-L, inverted-F, loop ("towel-bar"), and M antennas have been used to shift the resonance of the transmission line antennas. Also, other designs such as planar inverted-F antennas (PIFA) have been proposed in order to reduce the size and increase the bandwidth of the antenna.

Transmission line antennas were analytically analyzed by King and Harrison [1] who derived formulas for the driving point impedance of such elements. Also, Wunsch *et al*. were able to derive closed-form expressions for the driving point impedance of a small inverted-L antenna [2]. Even though transmission line antennas are widely used in today's communication systems, they have not been extensively discussed in the literature, especially in terms of analytical formulations and measurements. In this paper, the coupling between two transmission line elements such as loops and inverted-L's, is analytically formulated by using two different integral definitions of the mutual impedance. These two definitions of coupling form the basis of the *induced electromagnetic force (EMF) method*. All the analytical results are compared with numerical computations obtained by finite-difference time-domain (FDTD) and also with measurements. The theory of FDTD will not be discussed or illustrated here as it is well documented and has been successfully applied to a variety of problems. The FDTD method is based on Yee's algorithm [3] and is thoroughly examined in [4] and [5]. In this paper, an efficient technique that calculates the two-port network parameters of a system of two antennas is developed. Furthermore, the behavior of coupling is discussed and physical interpretations are provided.

Manuscript received May 12, 1998; revised January 4, 1999. This work was supported by the Advanced Helicopter Electromagnetics (AHE) Program and NASA Grant NAG-1-1082.

The authors are with the Department of Electrical Engineering, Telecommunications Research Center, Arizona State University, Tempe, AZ 85287 USA.

Publisher Item Identifier S 0018-926X(99)05804-4.

II. Definition of Mutual Coupling

The mutual coupling between two antennas was initially modeled using the Z parameters of the equivalent two-port network. Assuming that $I_1(0;s_1)$ is the current distribution in the first antenna due to an applied voltage at $s_1 = 0$ and $E_{s,1}(s_2)$ is the electric field intensity produced by this current along the second antenna, the mutual impedance Z_{12} between the two antennas is written as

$$Z_{12} = -\frac{1}{I_{i,1}I_{i,2}} \int_{s_{21}}^{s_{22}} E_{s,1}(s_2) I_2(0;s_2)\, ds_2 \tag{1}$$

where $I_2(0;s_2)$ is the current distribution in the second antenna due to an applied voltage across its terminals at $s_2 = 0$ and $I_{i,1}$ and $I_{i,2}$ are the input currents of the antennas. Equation (1) was first derived by Carter [6] and assumes that the field $E_{s,1}(s_2)$ is known.

Schelkunoff and Friis [7] generalized the definition of (1) by introducing one more integration in order to compute $E_{s,1}(s_2)$. Consider the free-space transmission factor $T(s_1, s_2)$ between two antenna elements ds_1 and ds_2, which is defined as the ratio of the electric field intensity at s_2 along the tangent to the element ds_2 to the moment of the current at s_1 flowing through the element ds_1. Then the electric field intensity $E_{s,1}(s_2)$ can be written as

$$E_{s,1}(s_2) = \int_{s_{11}}^{s_{12}} T(s_1, s_2) I_1(0;s_1)\, ds_1. \tag{2}$$

Consequently, the function T can be obtained from the electric field of an infinitesimal electric current element I_s. Finally, the generalized definition formula for the mutual coupling between two antenna elements is obtained by substituting (2) in (1)

$$Z_{12} = -\frac{1}{I_{i,1}I_{i,2}} \int_{s_{11}}^{s_{12}} \int_{s_{21}}^{s_{22}} T(s_1, s_2) I_1(0;s_1) \times I_2(0;s_2)\, ds_1\, ds_2. \tag{3}$$

This method that analytically computes coupling between two wire antennas and is described by (1) or (3) is referred to as

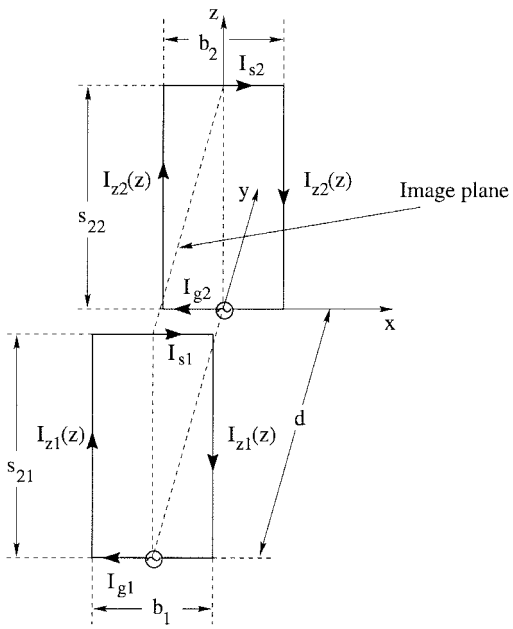

Fig. 1. Loop antennas and their images.

induced EMF method [8]. The accuracy of the first approach based on (1), depends on the knowledge of the electric field radiated by one antenna and the current distribution on the other antenna. However, the electric field radiated by complex wire antennas, especially in the near-field zone, is not usually known. On the contrary, the accuracy of the second approach, based on (3), depends only on the knowledge of the current distributions along the two antennas, which are usually known or easy to derive even for multijunction wire antennas.

III. Analytical Formulation of Coupling

In this section, the mutual coupling between two wire antennas is analytically formulated. The approach followed herein is based on the induced EMF method and involves either the single or double integration described by (1) and (3), respectively. The interference between wire antennas that are mounted on infinite ground planes can be analytically computed by using image theory. Therefore, by applying image theory a rectangular loop antenna becomes a two-wire short-circuited transmission line, and an inverted-L antenna becomes a two-wire open-circuited transmission line. It should be pointed out that the mutual impedance Z_{12} of two antennas placed on an infinite ground plane is equal to one-half of the Z_{12} of the equivalent problems computed by image theory. Furthermore, application of image theory in the case of finite ground planes should give fairly accurate results as the mutual coupling is not greatly influenced by the finite dimensions of the ground plane, provided the ground plane is not very small or the feed is not very near one of the edges.

A. Mutual Coupling Between Rectangular Loop Antennas

Two loop antennas along with their images are shown in Fig. 1. These configurations of the loops are often referred in practice as "towel bar" antennas and find wide application in airborne platforms such as helicopters, airplanes, missiles, etc. Obviously, a loop antenna becomes a short-circuited transmission line (SC-TL) antenna after the use of image theory. The mutual impedance between two SC-TL antennas will be computed in two ways.

The first approach is based on the assumption that one antenna is located at the far-field of the other antenna. Therefore, the electric field involved in (1) is the far-zone field of the SC-TL antenna. The electric field of a SC-TL antenna in the far-field can be deduced by the vector potential derived by King for a transmission line antenna [1]. A SC-TL antenna exhibits A_x and A_z components of the vector potential, as it consists of currents along the x and z directions. These two components A_x and A_z can be deduced from King's formulations. Additionally, the electric field components in the far field can be written in terms of the vector potential components as [8]

$$E_\theta \simeq -j\omega A_\theta \tag{4}$$

$$E_\phi \simeq -j\omega A_\phi. \tag{5}$$

However, the calculation of the mutual impedance involves the tangential components of the electric field to the branches of the SC-TL antenna, which are the E_x and E_z components. These Cartesian components can be computed by performing a coordinate transformation of the spherical components given by (4) and (5). Obviously, the integration of (1) can be separated into four integrals

$$I_1 = \int_0^{s_{22}} E_{z1} I_{z2}\, dz, \quad \text{at } y = d, \quad x = -b_2/2 \tag{6}$$

$$I_2 = \int_{s_{22}}^{0} E_{z1} I_{z2}\, dz, \quad \text{at } y = d, \quad x = b_2/2 \tag{7}$$

$$I_3 = \int_{b/2}^{-b/2} E_{x1} I_{g2}\, dx, \quad \text{at } y = d, \quad z = 0 \tag{8}$$

$$I_3 = \int_{-b/2}^{b/2} E_{x1} I_{s2}\, dx, \quad \text{at } y = d, \quad z = s_{22} \tag{9}$$

where E_{x1} and E_{z1} are the electric field components in the far-field zone of the first SC-TL antenna. Moreover, the integrations of (6)–(9) can be carried out numerically if the current distribution along a SC-TL antenna is known. Different current distributions of SC-TL antennas are examined later in this paper and their advantages and disadvantages are outlined.

The second approach for computing the mutual impedance between two loop antennas is based on (3), which consists of a double integration. In the case of SC-TL antennas, there are two transmission factors T_x and T_z, as currents exist along the x and z axes, respectively. The factor T_x expresses the field of an infinitesimal current element along the x axis, and T_z expresses the field of an infinitesimal current element along the z axis. Notice that the transfer function considers only the tangential components of the electric field to the wire antenna, which, in this case, are the E_x and E_z components. Therefore, the T_z function has two components namely T_{zx} and T_{zz} and the T_x function has also two components T_{xx} and T_{xz}. The mutual impedance of two loop antennas can be calculated from (3) by double integrating the product of the transfer functions and the currents of the respective SC-TL

antennas. The integration can be separated into 16 different integrals.

B. Mutual Coupling Between Inverted-L Antennas

The mutual coupling between two inverted-L antennas can be formulated following a similar procedure to the one illustrated for the loop antennas. The details of the formulation are described in [9].

IV. Current Distributions Along Transmission Line Antennas

The current distribution of a shunt-driven reactively terminated transmission line was developed by King [1]. In this paper, only loop and inverted-L antennas are examined. Their current distributions can be derived using either King's derivations or the transmission line theory for a short and open circuited lossless transmission line [10]. Moreover, additional terms in these current distributions are added to treat the parallel type of resonances (antiresonances).

A. Current Distribution of a Loop Antenna

Following either King's formulations or the transmission line theory for a short-circuited lossless transmission line, the current distribution along a loop antenna can be written as

$$I_z(z) = I_0 \cos[\beta(s_e - z)], \qquad 0 \le z \le s_e \tag{10}$$

$$I_g = I_z(0) = I_0 \cos(\beta s_e), \quad I_s = I_z(s_e) = I_0 \tag{11}$$

where s_2 is the actual length of the loop antenna, $h = b/2$ is its height, and $s_e = s_2 + h$ its effective length derived by King showed to account for the variation of the transmission line parameters, R, L, G, and C near the end of the line.

This current distribution can be used in conjunction with the induced EMF method to compute the self and mutual impedances of loop antennas. The accuracy of the results obtained by the induced EMF method, depends greatly on the accuracy of the current distribution. The current distribution of (10) gives accurate results at all frequencies, except the ones where the input current I_g becomes zero. This occurs when the effective length of the antenna s_e is an odd multiple of quarter-wavelength, i.e., $\cos(\beta s_e) = 0$; these frequencies correspond to the parallel resonances of the loop (antiresonances). Consequently, the division with the input currents, that is involved in (1) and (3) does not give valid results at the antiresonances of either antenna. This problem can be treated by adding a quadrature term that will prevent the current from vanishing. The approach illustrated below follows the approach presented by Friis and Schelkunoff [7] for dipole antennas. In order for the current on a loop not to vanish at its parallel resonances, an appropriate weighted sinusoidal term is added to the current distribution

$$I_z(z) \;=\; I_0 \cos[\beta(s_e - z)] + jpI_0 \sin(\beta s_e) \quad 0 \le z \le s_e \tag{12}$$

The only remaining task is to determine the values of the coefficient p. The input resistance R_i and the input reactance X_i of a SC-TL antenna were derived by King as

$$R_i = \frac{30\beta^2 b^2}{\cos^2(\beta s_e)}\left(1 - \frac{\sin(2\beta s_e)}{2\beta s_e}\right), \quad X_i =_c Z_o \tan(\beta s_e) \tag{13}$$

where Z_0 is the characteristic impedance of the two-wire transmission line model. The input resistance and reactance of a SC-TL antenna can be referred to the maximum current of a SC-TL antenna as follows:

$$R_i|I_i|^2 = R_a|I_0|^2, \quad X_i|I_i|^2 = X_a|I_0|^2 \tag{14}$$

where I_i is the input current and I_0 is the maximum current. Considering that the currents I_i and I_0 according to King's derivations are

$$I_i = I_g, \quad I_0 = \frac{I_g}{\cos(\beta s_e)} \tag{15}$$

the input resistance and reactance of a SC-TL antenna referred to the maximum current become

$$R_a = 30\beta^2 b^2\left(1 - \frac{\sin(2\beta s_e)}{2\beta s_e}\right), \quad X_a =_c Z_0 \sin(\beta s_e)\cos(\beta s_e). \tag{16}$$

The radiated power may be expressed in terms of either the input voltage or the maximum current as

$$P = \frac{1}{2} G_i V_i^2 = \frac{1}{2} R_a I_0^2 \tag{17}$$

where G_i is the input conductance, i.e., the reciprocal of the input resistance R_i and R_a is the radiation resistance. At resonance, the maximum stored magnetic energy $\mathcal{E}_m$ should be equal to the maximum stored electric energy $\mathcal{E}_e$. The loop antenna will be treated again as a short-circuited transmission line (SC-TL) antenna. Considering the first parallel resonance of the SC-TL antenna $s_e = \lambda/4$ the maximum magnetic energy can be obtained from

$$\mathcal{E}_m = \frac{1}{2} L \int_0^{\lambda/4} [I(z)]^2 \, dz = \frac{1}{16} L\lambda I_0^2 \tag{18}$$

where L is the wire inductance per unit length and $I(z)$ is the cosinusoidal current distribution along the antenna. Similarly, the maximum electric energy can be obtained from

$$\mathcal{E}_e = \frac{1}{2} C \int_0^{\lambda/4} [V(z)]^2 \, dz = \frac{1}{16} C\lambda V_i^2 \tag{19}$$

where C is the capacitance per unit length and $V(z)$ is the sinusoidal voltage distribution along the antenna. Equating the magnetic and electric energies, the following relation is obtained:

$$\frac{V_i}{I_0} = \sqrt{\frac{L}{C}} = Z_0. \tag{20}$$

Similarly, it can be shown that (20) holds at all the parallel resonances of the antenna. Furthermore, using (17) and (20), the input conductance can be written as

$$G_i = R_a \frac{I_0^2}{V_i^2} = \frac{R_a}{Z_0^2}, \qquad R_i = \frac{Z_0^2}{R_a}. \tag{21}$$

Combining (21) and (14), the following relationship is derived:

$$\frac{|I_i|}{|I_0|} = \sqrt{\frac{R_a}{R_i}} = \frac{R_a}{Z_0} \tag{22}$$

where R_a is the radiation resistance of a SC-TL antenna at its parallel resonances, i.e., $s_e = (2n+1)\lambda/4$, $n = 0, 1, 2\cdots$, which can be written according to (16) as

$$R_a = 30\beta^2 b^2. \tag{23}$$

Moreover, when the SC-TL antenna operates at one of its antiresonances, the corrected current distribution described by (12) becomes

$$I_i = jpI_0. \tag{24}$$

From (22)–(24) the coefficient p can be written as

$$p = \frac{R_a}{Z_0} = \frac{30\beta^2 b^2}{Z_0}. \tag{25}$$

Notice that (25) is correct only at the antiresonances of an SC-TL antenna. However, the standard current distribution is significantly affected by the correction term only at the antiresonances. Therefore, (25) can be used to provide values of p at all frequencies. Hence, the corrected current distribution can be written as

$$I_z(z) = I_0\cos[\beta(s_e - z)] + j\frac{30\beta^2 b^2}{Z_0} I_0 \sin(\beta s_e) \qquad 0 \le z \le s_e. \tag{26}$$

Furthermore, the input resistance of a SC-TL antenna, referred to the corrected current at the input terminal, can be deduced from (14) and (16), i.e.,

$$R_i = 30\beta^2 b^2\left(1 - \frac{\sin(2\beta s_2)}{2\beta s_2}\right)\frac{|I_0|^2}{|I_i|^2}$$
$$X_i = {}_cZ_0 \sin(\beta s_e)\cos(\beta s_e)\frac{|I_0|^2}{|I_i|^2} \tag{27}$$

where I_i is the corrected input current of the SC-TL antenna given by

$$I_i = I_z(0) = I_0\cos(\beta s_e) + j\frac{30\beta^2 b^2}{Z_0} I_0 \sin(\beta s_e). \tag{28}$$

Notice that the input resistance and reactance of a loop antenna is equal to one-half of the input resistance and reactance of the corresponding SC-TL antenna given by (27).

B. Current Distribution of an Inverted-L Antenna

The formulation of the current distribution of an inverted-L antenna is not described here as it follows similar methodology with the loop antenna [9]. Note, that the derivation of the corrected current distribution for an inverted-L differs to that of the loop only in the fact that the inverted-L exhibits a sinusoidal current distribution.

V. Efficient Computation of Two-Port Network Parameters

The computation of the input impedance of an antenna or the network parameters of a system of antennas by FDTD involves the Fourier transform of the input voltages and currents. Therefore, using a transient excitation (pulse) the impedance or the network parameters can be determined over a frequency band by fast Fourier transforming (FFT) the time-domain data. The basic requirement for the FFT to work is to allow enough simulation time for the transient phenomena to decay. However, one of the main difficulties involved in FDTD simulations is that in some applications, e.g., resonant lossless structures, tens or even hundreds of thousands of time steps may be required for the transient fields to decay.

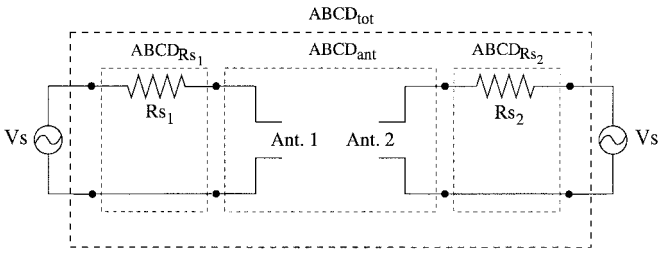

Fig. 2. Augmented system of two generic antennas with voltage sources.

A novel, effective, and very simple excitation technique to implement for reducing the FDTD simulation time is based on a source with an internal resistance. Initially, this method was used in [11] to excite microstrip patch antennas. In addition, the expression for a voltage source with an internal resistance in parallel with the free-space capacitance of the FDTD cell is given in [12]. However, the advantages of this method were illustrated and outlined explicitly only in [13]. Besides, when a problem involves the calculation of the network parameters of a system of antennas, then a modified approach should be used. The augmented system of two generic antennas along with the voltage sources is shown in Fig. 2. This system can be thought of as the cascade connection of three two-port networks, as illustrated in Fig. 2.

The proposed approach requires to initially compute the Y parameters of the entire system including the antennas and the load resistors. Then, the Y parameters of the system are converted to ABCD parameters. It can be readily shown that the ABCD matrix of the overall antenna system $\mathrm{ABCD}_{\mathrm{ant}}$ can be computed by the following expression:

$$\begin{bmatrix} A_{\mathrm{ant}} & B_{\mathrm{ant}} \\ C_{\mathrm{ant}} & D_{\mathrm{ant}} \end{bmatrix} = \begin{bmatrix} A_{R_{s1}} & B_{R_{s1}} \\ C_{R_{s1}} & D_{R_{s1}} \end{bmatrix}^{-1} \begin{bmatrix} A_{\mathrm{tot}} & B_{\mathrm{tot}} \\ C_{\mathrm{tot}} & D_{\mathrm{tot}} \end{bmatrix} \times \begin{bmatrix} A_{R_{s2}} & B_{R_{s2}} \\ C_{R_{s2}} & D_{R_{s2}} \end{bmatrix}^{-1}. \tag{29}$$

The computed $\mathrm{ABCD}_{\mathrm{ant}}$ matrix of the two antennas can be converted (if needed) to any other type of two-port network parameters using the appropriate conversion formulas. Following the method described, computation of the ABCD parameters of the two antennas can lead to great savings in the computational time.

VI. Discussion on the Behavior of Mutual Coupling

Here the coupling between two side-by-side dipoles is examined in order to discuss the physics of coupling between wire elements and draw some general conclusions. The admittance (Y) parameters can be used to model the two dipoles as a two-port network. The mutual admittances Y_{12} and Y_{21}, which express the coupling between the two dipoles, are equal for reciprocal systems. The mutual admittance Y_{21} is chosen to be used in the following formulation. Using the sinusoidal current distribution for a very thin dipole [8] (ideally zero diameter) along with the definition of the Y parameters it can

be shown that the mutual admittance $Y_{21}(\omega)$ can be written as

$$Y_{21}(\omega) = \left[\frac{I_{02}(\omega)}{I_{01}(\omega)}\bigg|_{V_2=0}\right] Y_{11m}(\omega)\sin\left(\frac{\beta l_1}{2}\right)\sin\left(\frac{\beta l_2}{2}\right) \tag{30}$$

where $Y_{11m}(\omega)$ is the self admittance of antenna 1 referred to the current maximum and $I_{01}(\omega)$ and $I_{02}(\omega)$ are the amplitudes of the sinusoidal current distributions of the dipoles. A similar expression for $Y_{12}(\omega)$ can also be derived. It can be concluded from (30) that the coupling between the two dipoles depends on $Y_{11m}(\omega)$ and the factor $\sin(\frac{\beta l_1}{2})\sin(\frac{\beta l_2}{2})$. Therefore, the coupling can be intense if $Y_{11m}(\omega)$ is large; i.e., antenna 1 operates near one of its odd resonances, or if the product of the sinusoids is large. The sinusoid $\sin(\frac{\beta l_1}{2})$ peaks when the length of antenna 1 is an odd multiple of half-wavelength, i.e., antenna 1 operates at one of its odd resonances (or series resonances). Similarly, the sinusoid $\sin(\frac{\beta l_2}{2})$ peaks when antenna 2 operates at one of its odd resonances. Combining the above, the factor $\sin(\frac{\beta l_1}{2})\sin(\frac{\beta l_2}{2})$ may peak when the operating frequency is close to one of the odd resonances of either antenna. However, if one of the antennas operates at one of its even resonances (or parallel resonances) then its respective sinusoidal term vanishes and therefore the coupling $Y_{12}(\omega)$ or $Y_{21}(\omega)$ also vanishes. Summarizing, the interference between the two dipoles can be intense if the operating frequency is near one of the odd resonances of either antenna. Another important conclusion is that the factor of the two sinusoids describes the behavior of coupling.

The conclusions asserted by this example can be generalized for any kind of antenna. An antenna has two types of resonances: the series and the parallel type of resonances. The series type of resonances are more broad band than the parallel type of resonances (antiresonances), and they are much easier to match as they exhibit input resistances close to the characteristic impedances of standard transmission lines. On the contrary, the antiresonances are extremely narrow band and exhibit very large values of input resistances that are difficult to match with practical transmission lines. Consequently, an antenna usually is operated at one of its series resonances where it provides a good match to a transmission line and, therefore, can radiate efficiently. Thus, if no coupler is used to match an antenna to its feeding transmission line, the antenna will radiate effectively only at or near its series resonances. Moreover, when an antenna operates at one of its antiresonances, it does not only transmit power inefficiently, but also receives inefficiently, according to reciprocity theorem. Therefore, it can be concluded that the coupling between two antennas that are connected directly to their transmission lines (no matching circuit is used) can be intense at or near one of the series type of resonances of either antenna, provided it is not near an antiresonance of the other. On the contrary, the coupling between such antennas is low at or near one of the antiresonances of either antenna, independently of the electrical length of the other. These conclusions are very important because they describe the behavior of coupling and predict the locations of possible peaks and nulls.

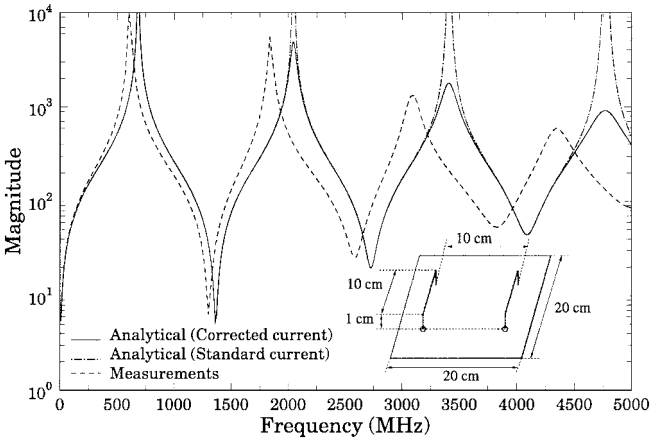

(a)

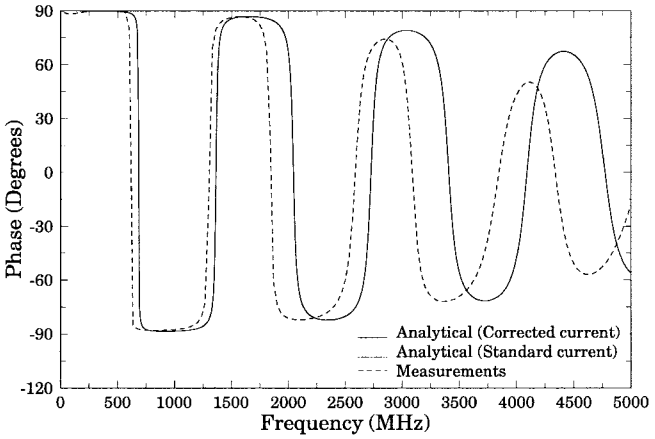

(b)

Fig. 3. Input impedance of two identical loop antennas. (a) Magnitude. (b) Phase.

VII. Results

A. Loop Antennas on Ground Planes

Loop antennas are widely used transmission line antennas. In this section, the mutual coupling between two loops is analytically computed. Moreover, the analytical results are compared with the corresponding FDTD calculations and measurements. In order to validate our approach, a geometry of two identical loops mounted on a finite ground plane (often referred to in practice as "towel bar" antennas) is initially examined (see Fig. 3). The two loops are 10 cm long, placed 1 cm above the ground plane, the distance between them is 10 cm and their wire radius is 0.4 mm.

First, FDTD was used to calculate the Y parameters of the two loops without any modeling of their wire radius. Loop antennas are extremely resonant as they exhibit a short-circuited end. Therefore, a voltage source with an internal resistance $R_s = 50\,\Omega$ was used in order to calculate efficiently the Y parameters of the two antennas and reduce substantially the computation time. In the FDTD simulation the cell size was 2 mm, the computational space was $120 \times 120 \times 26$ cells, and the computational time was 4 000 time steps. The Y parameters were converted to S parameters by assuming that the characteristic impedance of the transmission line is 50 Ω.

In order to compare the accuracy of the different current distributions, i.e., standard versus corrected, the analytically computed input impedance of the two identical loops is compared with measurements in Fig. 3. The magnitude of the input impedance computed using the standard current distribution blows up at the antiresonances of the loops whereas the corrected one provides levels that remain finite and close to the measured ones [see Fig. 3(a)]. On the other hand, the phase of the input impedance is the same for both current distributions as the resonant frequencies are the same for both of them [see Fig. 3(b)]. Notice, that the analytically computed input impedance does not agree very well with the measurements at the higher frequency band and the resonances are shifted. This error is attributed to the formulas derived by King that compute the self impedance of a loop and will be readily explained later in this section. It should be emphasized that although the analytical calculations apply image theory, i.e., infinite ground plane, that does not significantly affect their accuracy because the input impedance is not strongly influenced by the ground plane dimensions as other antenna characteristics such as the patterns.

Additionally, the coupling between the two loops was analytically computed by three different approaches by assuming that the ground plane is infinite. The radius of the wires was taken into account only in the computation of the characteristic impedance Z_0 in (20). The first approach is based on the assumption that one of the loops is located at the far-field zone of the other loop and their mutual impedance was computed as described in Section III. The second approach uses the near fields produced by the loops in order to calculate more accurately the mutual impedance and it is also discussed in Section III. In both approaches the current distribution of (10) (which vanishes at the antiresonances of either loop) was used and the self impedances were calculated by the formulas derived by King. The third approach computes the mutual impedance by using the near-field formulation along with the corrected current distribution of (26) that is valid at all frequencies. Moreover, the self impedances of the loops were calculated by referring them to the corrected input current as presented in Section IV. All the integrations involved in the calculation of the mutual impedance were carried out numerically by using a 16-point Gaussian quadrature.

Fig. 4(a) illustrates the results of the first two analytical approaches and compares them with the FDTD calculations and measurements. Obviously, the FDTD results exhibit excellent agreement with measurements. Moreover, the S_{12} parameter computed by the analytical far-field method does not agree very well with the measured data. However, as expected, the analytical near-field method gives improved accuracy and compares fairly well with measurements. The discrepancy between measured and analytically computed coupling is more profound at the higher end of the band and is due to the shift of the analytically predicted resonances of the loops (see Fig. 3). As already stated above, the source of this error will be identified later this section. Furthermore, the analytical solutions based on the noncorrected current distribution do not give valid results at the antiresonances of the loop antennas [observe the deep nulls in Fig. 4(a)]. On the contrary, when the near-field

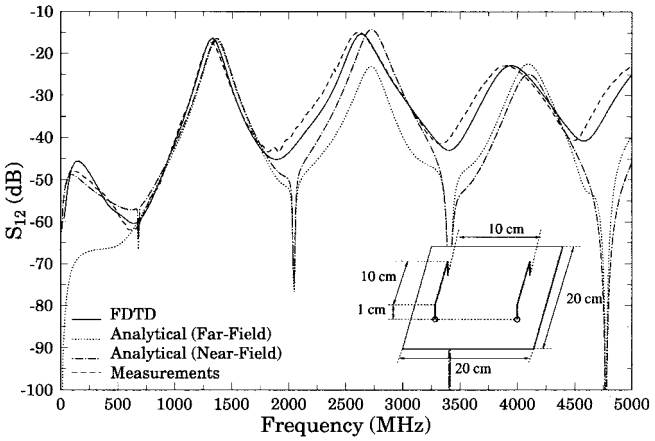

(a)

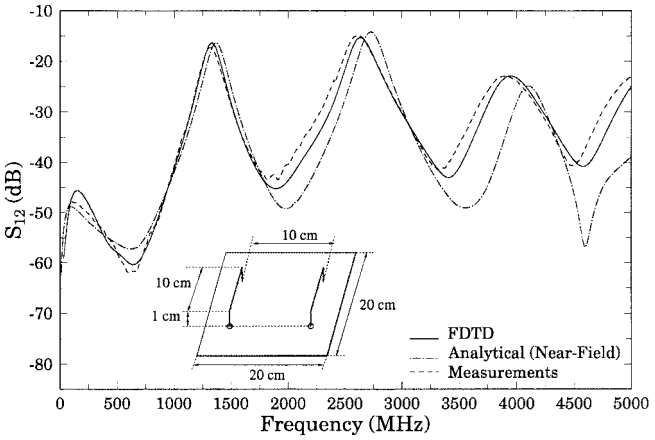

(b)

Fig. 4. S_{12} of two identical loop antennas. (a) Standard current distribution. (b) Corrected current distribution.

method is used along with the corrected current distribution it leads to valid results at all frequencies as it does not vanish at the antiresonances. The calculations of this method along with the FDTD results and measurements are demonstrated in Fig. 5(b). Evidently, the near-field method combined with the corrected current distribution is the most accurate approach of the three analytical methods. It should be also pointed out that the two methods (far-field and near-field methods) that use the standard current distribution cannot be applied to accurately compute coupling between two unequal loop antennas. In such a case, the resonances of the antennas will be different; thereby, invalid results will be obtained at the antiresonances of either antenna. Therefore, the results will be greatly disturbed at and near these frequencies yielding poor accuracy at a substantial part of the bandwidth under examination.

After validating our procedure and establishing the most accurate way to analytically compute coupling, the geometry of two different loop antennas, shown in Fig. 5(a), was analyzed. The S parameters were computed by FDTD following a procedure similar to the previous case. All the simulation parameters, including cell size and total number of time steps, were the same as previously. In addition, the mutual impedance of the two loops was analytically computed by combining the near field method with the corrected current

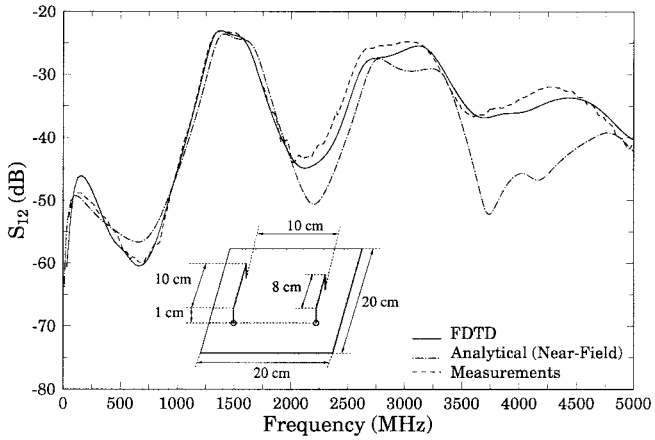

(a)

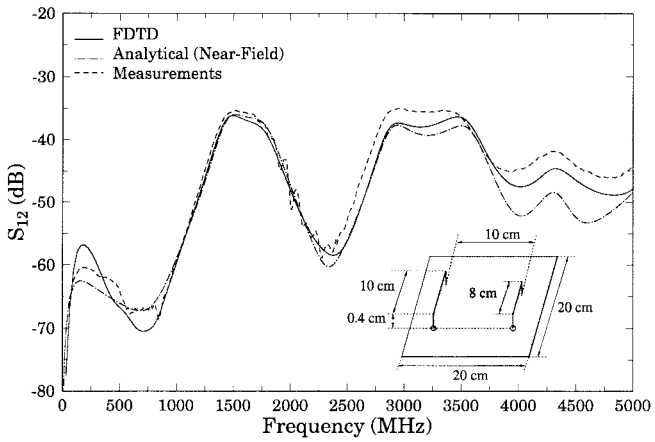

(b)

Fig. 5. S_{12} of two loop antennas. (a) Legs 10 mm long. (b) Legs 4 mm long.

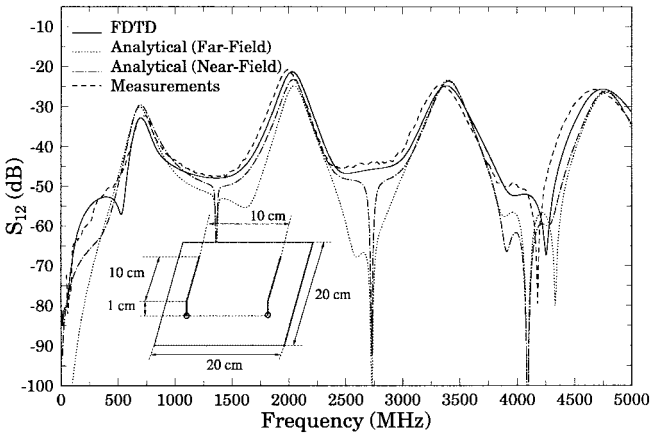

(a)

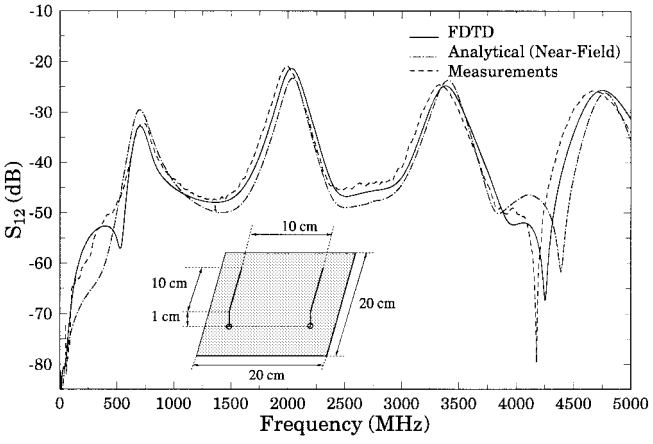

(b)

Fig. 6. S_{12} of two identical inverted-L antennas. (a) Standard current distribution. (b) Corrected current distribution.

distribution. The analytically computed S_{12} is illustrated in Fig. 5(a) along with the FDTD results and the measurements. Obviously, the FDTD computations compare very well with the measurements. Also, the agreement between the analytical and measured data is very good in the lower frequency band, but it deteriorates at the higher band. This can be partially attributed to the failure to predict accurately the resonances of each antenna at the higher frequencies. It should be pointed out that King derived the current distribution of a loop antenna based on the assumption that the length of its two legs is small compared to the wavelength. This assumption assures that the current along the two legs is constant. However, in the geometry analyzed above, the length of the legs of the loop is 1 cm or $\lambda/6$ at 5 GHz. Therefore, at the frequencies close to 5 GHz, the length of the legs is comparable to the wavelength. This fact causes the disagreement exhibited mainly at the higher end of the band, between the analytical and the measured data.

To verify our interpretation, another geometry was analyzed. This geometry was exactly the same as the one illustrated in Fig. 5(a) except that the length of the legs of the loops was smaller; the legs were 4 mm long (2.5 times smaller than before). Fig. 5(b) shows the analytically computed S_{12} parameter for the second geometry and compares it with the FDTD results and measurements. It is evident that the agreement between the analytical results and the measurements becomes better as the length of the legs of the loops becomes smaller. Consequently, it is suggested that the analytical procedure should be used to compute the S parameters between two loops only when the length of the legs of the loops is small compared to the wavelength.

B. Inverted-L Antennas on Ground Planes

Inverted-L antennas are widely used transmission line antennas. In this section, mutual coupling between two inverted-L's is analytically computed. Additionally, the analytical computations are compared with the respective FDTD results and measurements. A geometry of two identical inverted-L's 10 cm long placed 1 cm above a finite ground plane is examined here (see Fig. 6). The distance between them is 10 cm and their wire radius is 0.4 mm.

First, FDTD was used to calculate the Y parameters of the two inverted-L's. The procedure followed to compute the coupling as well as the simulation parameters were the same with the ones described in the analysis of the loops. In addition, the analytical computations were performed for the same three cases as for the identical loop antennas, namely: a) far-field approach with standard current distribution and b) and c) near-field approach for standard and corrected current distributions,

respectively. The analytical calculations along with the FDTD results and the measurements are demonstrated in Fig. 6.

VIII. Conclusion

In this paper, the coupling between transmission line type of antennas, such as loops and inverted-L's, was analytically formulated. The analytical formulations were based on different definitions of coupling and the use of image theory. The definition of coupling as derived by Carter is not very useful as it requires the knowledge of the field radiated by one of the antennas. However, the definition of coupling by Schelkunoff and Friis is more versatile as it requires only the knowledge of the current distributions along the two antennas. Furthermore, corrected current distributions that exhibit nonzero input current at the antiresonances of such antennas were developed in order to compute accurately the coupling between such elements at all frequencies. The coupling between two loop or inverted-L antennas was computed analytically and by FDTD. The FDTD results always exhibited excellent agreement with the measurements. Also, the analytical computations compared fairly well with the FDTD and measured data. Notice, that these formulations can be easily extended to analytically formulate the coupling between any type of transmission line antennas, e.g., inverted-F's, M antennas, etc. By formulating the coupling between two dipoles, the physics of coupling was discussed and conclusions for the general behavior of coupling were drawn. It was shown that the coupling between two antennas depends on the electrical length of either element. An interesting observation is that the series type of resonances of a loop are the antiresonances of the equal length inverted-L and vice versa. Combining this fact with the discussion on the physics of coupling (see Section VI) can explain why the peaks and nulls illustrated in Figs. 4 and 6 alternate frequency positions. Also, an efficient technique for calculating the two-port network parameters of a system of two antennas was developed.

References

[1] R. W. King and C. W. Harrison, *Antennas and Waves*. Cambridge, MA: MIT Press, 1969.

[2] A. D. Wunsch and S.-P. Hu, "A closed-form expression for the driving-point impedance of the small inverted L antenna," *IEEE Trans. Antennas Propagat.*, vol. 44, pp. 236–242, Feb. 1996.

[3] K. S. Yee, "Numerical solution of initial boundary value problems involving Maxwell's equations in isotropic media," *IEEE Trans. Antennas Propagat.*, vol. AP-14, pp. 302–307, May 1966.

[4] A. Taflove, *Computational Electrodynamics: The Finite-Difference Time-Domain Method*. Boston, MA: Artech House, 1995.

[5] K. S. Kunz and R. J. Luebbers, *The Finite Difference Time Domain Method for Electromagnetics*. Boca Raton, FL: CRC, 1993.

[6] P. S. Carter, "Circuit relations in radiating systems and application to antenna problems," *Proc. IRE*, vol. 25, pp. 1004–1041, June 1932.

[7] S. A. Schelkunoff and H. T. Friis, *Antennas-Theory and Practice*. New York: Wiley, 1952.

[8] C. A. Balanis, *Antenna Theory: Analysis and Design*. New York: Wiley, 1997.

[9] S. V. Georgakopoulos, "Coupling between multiple wire antennas on complex structures," M.S. thesis, Arizona State University, Tempe, 1998.

[10] D. M. Pozar, *Microwave Engineering*. Reading, MA: Addison-Wesley, 1990.

[11] A. Reineix and B. Jecko, "Analysis of microstrip patch antennas using finite difference time domain method," *IEEE Trans. Antennas Propagat.*, vol. 37, pp. 1361–1369, Nov. 1989.

[12] M. Piket-May, A. Taflove, and J. Baron, "FD-TD modeling of digital signal propagation in 3-D circuits with passive and active loads," *IEEE Trans. Microwave Theory Tech.*, vol. 42, pp. 1514–1523, Aug. 1994.

[13] R. J. Luebbers and H. S. Langdon, "A simple feed model that reduces time steps needed for FDTD antenna and microstrip calculations," *IEEE Trans. Antennas Propagat.*, vol. 44, pp. 1000–1005, July 1996.

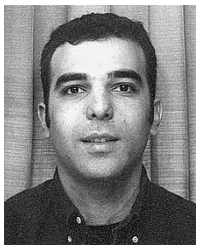

Stavros V. Georgakopoulos (S'93) was born in Athens, Greece, in May 1973. He received the Diploma (electrical engineering) degree from the University of Patras, Greece, in 1996, and the M.S. (electrical engineering) degree from Arizona State University (ASU), Tempe, in 1998. He is currently working toward the Ph.D. degree in electrical engineering at ASU with a concentration in the area of computational and applied electromagnetics in radiation and scattering problems.

In August 1996, he joined the Telecommunications Research Center (TRC), ASU. Since then, he has been working as a Graduate Research Assistant in computational electromagnetics for the Advanced Helicopter Electromagnetics (AHE) Program.

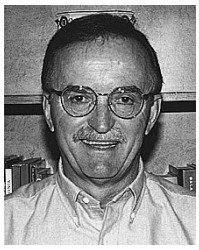

Constantine A. Balanis (S'62–M'68–SM'74–F'86) received the B.S.E.E. degree from Virginia Tech, Blacksburg, in 1964, the M.E.E. degree from the University of Virginia, Charlottesville, in 1966, and the Ph.D. degree in electrical engineering from Ohio State University, Columbus, in 1969.

From 1964 to 1970, he was with NASA Langley Research Center, Hampton VA, and from 1970 to 1983 he was with the Department of Electrical Engineering, West Virginia University, Morgantown. Since 1983 he has been with the Department of Electrical Engineering, Arizona State University, Tempe, AZ, where he is now Regent's Professor and Director of the Telecommunications Research Center. He is the author of *Antenna Theory: Analysis and Design* (New York: Wiley, 1997; 1982) and *Advanced Engineering Electromagnetics* (New York: Wiley, 1989). His research interests are in low- and high-frequency computational methods for antennas, scattering, and penetration; transient analysis, control of coupling, and reduction of pulse distortion in interconnects for monolithic microwave and millimeter-wave circuits; modeling of electronic packages for microwave, millimeter wave, and high-speed high-density integrated circuits; and multipath propagation.

Dr. Balanis received the 1992 Special Professionalism Award from the IEEE Phoenix Section, the 1989 IEEE Region 6 Individual Achievement Award, the 1996 Arizona State University Outstanding Graduate Mentor Award, and the 1987–1988 Graduate Teaching Excellence Award, School of Engineering, Arizona State University. He has served as Associate Editor of the IEEE Transactions on Antennas and Propagation (1974–1977) and the IEEE Transactions on Geoscience and Remote Sensing (1981–1984). He was also Editor of the Newsletter for the IEEE Geoscience and Remote Sensing Society (1982–1983). He served as Second Vice-President (1984), member of the Administrative Committee (1984–1985) of the IEEE Geoscience and Remote Sensing Society, Chairman of the Distinguished Lecturer Program of the IEEE Antennas and Propagation Society (1988–1991), and member of the AdCom (1992–1995, 1997–1999) of the IEEE Antennas and Propagation Society. He is a member of ASEE, Sigma Xi, Electromagnetics Academy, Tau Beta Pi, Eta Kappa Nu, and Phi Kappa Phi.

Craig R. Birtcher was born in Phoenix, AZ, on March 30, 1959. He received the B.S. and M.S. degrees, both in electrical engineering, from Arizona State University, Tempe, in 1983 and 1992, respectively.

He has been with Arizona State University since 1987 and is currently an Associate Research Specialist in charge of the ElectroMagnetic Anechoic Chamber (EMAC) facility. His research interests include antenna and RCS measurement techniques, NF/FF techniques, and the measurement of electrical properties of solids.